Ru-Bipyridine Entrapped in the Supercages of EMC-1 Faujasite as Catalyst for the Trifluoromethylation of Arenes

Vincent Lemmens, Christophe Vos, Aram L. Bugaev, Jannick Vercammen, Niels Van Velthoven, Jorge Gascon, and Dirk E. De Vos*

Cite This: https://doi.org/10.1021/acsami.1c19655

Read Online

ACCESS | 📊 Metrics & More | 📖 Article Recommendations | 🔲 Supporting Information

ABSTRACT: Trifluoromethyl (CF_3) groups are versatile structural motifs especially in the field of agrochemicals and pharmaceuticals. However, current trifluoromethylation reactions are generally associated with stoichiometric amounts of transition metals/metal oxidants, homogeneous catalysts, high temperatures, and expensive trifluoromethylating agents. In this work, the homogeneous photocatalyst $Ru(bipy)_3^{2+}$ is entrapped in the pores of a faujasite support (EMC-1) via a "ship-in-a-bottle" strategy. The formation of the coordination compound was confirmed by Fourier transform infrared (FTIR), UV–Vis spectroscopy, and X-ray absorption spectroscopy (XAS). Due to its high stability toward acidified environments, this single-site heterogeneous catalyst is suitable for the trifluoromethylation of synthetically interesting (hetero)arenes under visible-light irradiation at room temperature. Furthermore, the heterogeneous catalyst could efficiently be reused for at least three times with minimal catalyst leaching/deactivation.

KEYWORDS: trifluoromethylation, photocatalysis, heterogeneous catalysis, $Ru(bipy)_3^{2+}$, faujasite
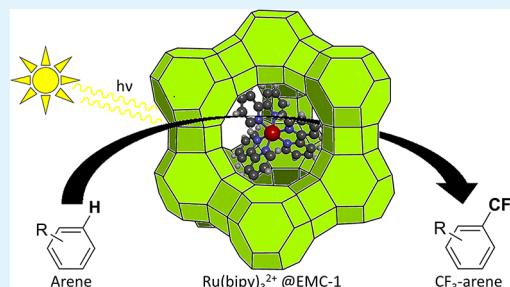
INTRODUCTION

Over the past decades, the synthesis of trifluoromethylated compounds has attracted much attention since this CF_3 entity is abundantly present in pharmaceuticals, agrochemicals, and organic functional materials.[1−3] More recently, a remarkable increase in FDA-approved drug molecules containing a CF_3 group is noticed[4] because this functional group significantly enhances molecular properties such as binding selectivity, lipophilicity, and metabolic/chemical stability.[1,3,5]

The CF_3 moiety is typically installed on arenes via a cross-coupling reaction that requires stoichiometric amounts of homogeneous organometallic complexes/metal oxidants at elevated temperatures (Figure 1, top).[6] Moreover, corrosive and expensive nucleophilic, electrophilic, or radical CF_3 sources are frequently used (e.g., CF_3I,[7,8] Togni,[9,10] Umemoto,[10] or Ruppert−Prakash[11] reagents). In recent years, photoredox catalysis has emerged as a promising alternative since it can be more environmentally and economically friendly. In this context, Macmillan investigated a mild and efficient method for creating electrophilic °CF_3 radicals using polypyridyl organometallic photoredox catalysts such as tris(1,10-phenanthroline)ruthenium(II) dichloride $(Ru(phen)_3Cl_2)$, tris(2,2′-bipyridine)ruthenium(II) dichloride $(Ru(bipy)_3Cl_2)$, or tris[2-(2,4-difluorophenyl)pyridine]-iridium(III) $(Ir(Fppy)_3)$.[6,12] The reaction is performed under visible light at room temperature, providing a strongly reducing catalyst $(*Ru(bipy)_3^{2+})$ that is able to activate more economically interesting CF_3 sources such as CF_3SO_2Cl
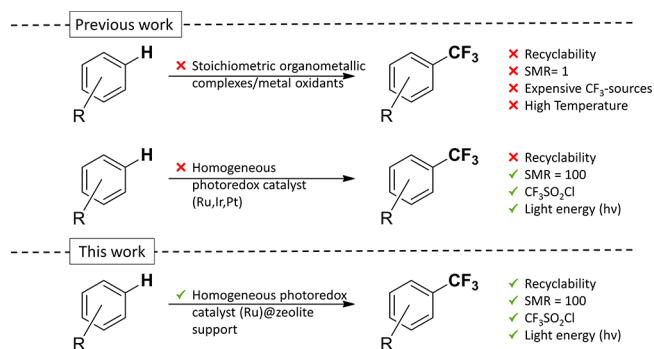
Figure 1. Different approaches to the generation of trifluoromethylated products starting from an arene. Usage of stoichiometric amounts of transition metals (TMs) or metal oxidants at elevated temperature with expensive CF_3 sources (top). A homogeneous photocatalytic approach with organometallic complexes (Ru, Ir, or Pt) and CF_3SO_2Cl (middle) and this work, where the reaction is catalyzed by a single-site heterogeneous catalyst under visible-light irradiation with CF_3SO_2Cl (bottom). SMR, substrate over metal ratio.
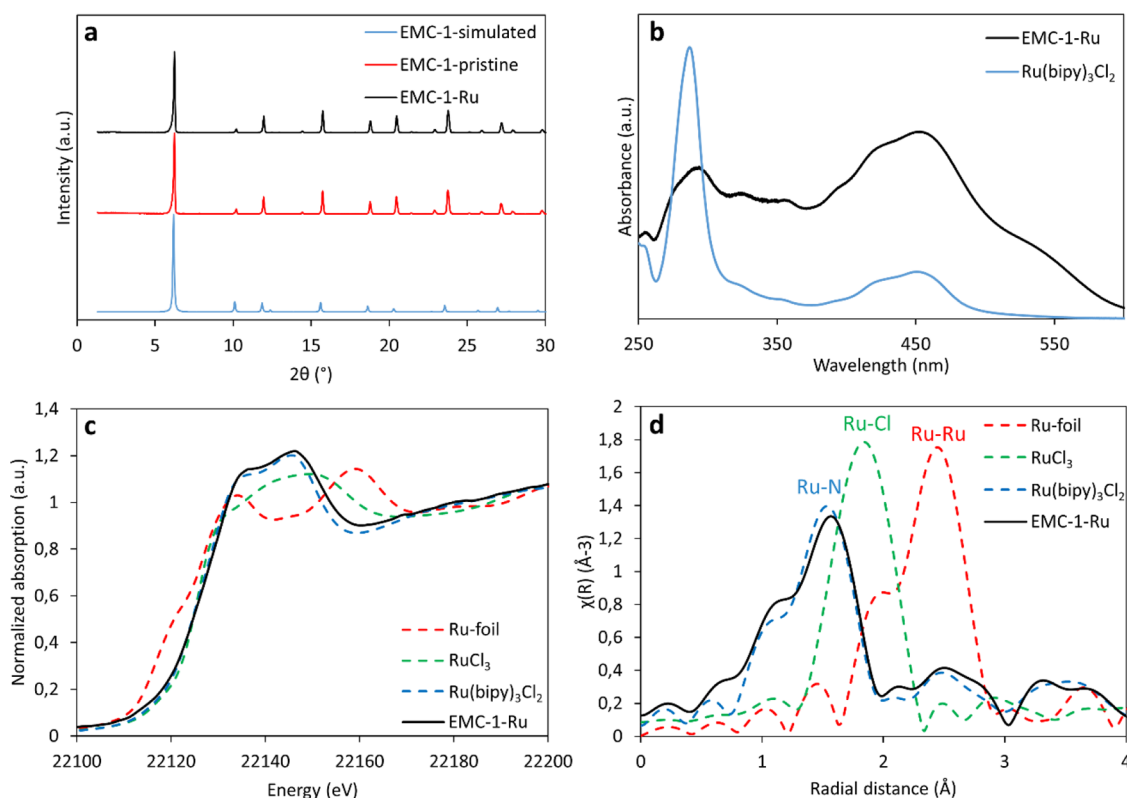
Figure 2. (a) XRD diffractogram of simulated EMC-1 (blue), synthesized pristine EMC-1 (red), and EMC-1-Ru (black). (b) UV−Vis spectrum of the homogeneous complex in acetonitrile ($Ru(bipy)_3Cl_2$, blue) and a diffuse reflectance spectrum of the Ru-loaded zeolite (black). (c, d) XANES (c) and EXAFS (d) data for EMC-1-Ru (solid black) in comparison with reference samples (dashed lines): $Ru(bipy)_3Cl_2$, blue; $RuCl_3$, green; Ru-foil, red.

(Figure 1, middle).[13−15] Nevertheless, the high cost and the laborious postsynthetic removal of the homogeneous photoactive catalysts hamper their further application in large-scale processes. Heterogeneous catalysts such as metal oxides,[2,16] carbon nitrides,[17] MOFs, and zeolites are typically considered as promising alternatives, but they have rarely been studied for photodriven trifluoromethylation.

Faujasite-type zeolite Y materials are aluminosilicates forming three-dimensional crystalline networks with tridirectional uniform pores/channels. These materials are of great interest in industrial processes and had a market value of USD 60 million in 2019[18] due to their low cost, shape/size selectivity, high stability, and high specific surface area (SSA).[19] Additionally, the ability to exchange transition metals is important for catalytic applications since these metal ions can act as the active site, forming a so-called single-site heterogeneous catalyst. Besides ion exchange, the supercages, communicated by smaller windows, of zeolite Y can be used to entrap organometallic complexes, offering a very elegant way for the creation of single-site heterogeneous catalysts. The use of zeolites as hosts for specifically photosensitizers also brings along other important features such as the ability to participate in electron transfer (ET) via the framework either as an electron acceptor or electron donor.[19−24] Moreover, zeolite supports are transparent to UV−Vis radiation above 240 nm, allowing the penetration of incoming light.[19,25]

In this work, a photoactive polypyridyl complex, $Ru(bipy)_3^{2+}$, is synthesized within the supercages of the faujasite type zeolite Y via a "ship-in-a-bottle" method to produce a single-site heterogeneous catalyst.[26] The entrapped Ru-complex can be excited by visible light to activate CF_3SO_2Cl (Figure 1, bottom), thereby avoiding the need for stoichiometric amounts of organometallic complexes/external oxidants.

■ RESULTS AND DISCUSSION

Synthesis of the Single-Site Heterogeneous Catalyst. Conventional faujasite-type zeolite Y materials, with a silicon-to-aluminum ratio (SAR) of about 2.5, suffer from instability toward acidic environments, which could result in crystallinity loss. Dealumination of the zeolite by chemical or hydrothermal treatment is a proven strategy to alleviate this limitation. However, these methods require laborious post-treatments such as steaming, acid leaching, filtration, drying, and washing. Moreover, a partially dealuminated material contains abundant defects, which could be the starting point for further Al removal and even structure loss upon contact with liquid acids. More recently, a direct one-step synthesis method was discovered by Patarin et al. to produce a faujasite-type zeolite Y with increased Si/Al ratio, EMC-1 [$Si_{3.6}Al_1O_{9.2}Na_1$ − SAR = 3.6].[27] In this procedure, the EMC-1 material is directly synthesized by using a structure-directing agent (e.g., 15-crown-5 ether) in a synthesis hydrogel. This EMC-1 zeolite has the same topology as the conventional faujasite-type zeolite Y and is therefore chosen as support material to introduce $Ru(bipy)_3^{2+}$ via a ship-in-a-bottle strategy.[26] The obtained EMC-1 material was generally ion-exchanged with 0.33 wt % Ru as $Ru(NH_3)_6Cl_3$ in Milli-Q water and afterward contacted with an excess of molten bipy to form the active complex in the 13 Å wide supercages. The resulting complex is too large to be

released through the 7.4 Å wide cage aperture (Figure S2).[25,26,28] The amount of entrapped photoactive molecules was determined by inductively coupled plasma atomic emission spectroscopy (ICP-OES) after the material was digested in aqua regia and HF (Table S1). Following the optimal synthesis procedure,[26,28] approximately 5% of the supercages contained the Ru complex, leading to the single-site heterogeneous catalyst EMC-1-Ru [$Si_{3.6}Al_1O_{9.2}Na_{0.99}$(Ru-$(bipy)_3^{2+})_{0.01}$]. The structure and crystallinity of the pristine and the functionalized zeolite (EMC-1-Ru) were confirmed by powder X-ray diffraction (PXRD) (Figure 2a), while scanning electron microsocopy images (SEM and SEM-EDX) revealed octahedral crystals of approximately 1.9 μm in diameter (Figures S3 and S4).

The incorporation of the Ru(bipy)$_3^{2+}$ into the supercages was further spectroscopically validated. Fourier-transform infrared spectroscopy (FTIR) data confirmed the presence of Ru(bipy)$_3^{2+}$ based on the characteristic bands in the region 1400 to 1500 cm^{-1}, which are associated to the C−C and C−N stretch vibrations and/or the C−H in-plane bend of the 2,2′-bipyridine ligand (Figure S5).[29,30] Furthermore, an absorption spectrum (Figure 2b) was collected for Ru(bpy)$_3^{2+}$ containing an absorption band with a maximum at 451 nm, which is attributed to the metal-to-ligand charge transfer (MLCT) from the d-orbital of Ru to the π*-orbital of the bipyridine ligand.[30,31] The EMC-1-Ru, measured in diffuse reflectance mode, had a similar absorption pattern with a maximum at 453 nm, leading to the excitation of the photocatalyst in the visible-light region. Additionally, band gap calculations (via the Kubelka−Munk theory) from the UV−Vis data indicated that the HOMO−LUMO gap of the Ru-loaded material (2.6 eV) is in line with the MLCT of the homogeneous complex (Figure S6).[31]

The oxidation state of the Ru center is of utmost importance, since only Ru(II) is susceptible to photoexcitation and can catalyze the trifluoromethylation reaction. The X-ray absorption near-edge structure (XANES) of the functionalized material confirms that the pattern of the encapsulated Ru is very similar to Ru(bipy)$_3$Cl$_2$, which is a first indication that the trivalent ruthenium atom from Ru(NH$_3$)$_6$Cl$_2$ is reduced to Ru(II) after the ship-in-a-bottle procedure (Figure 2c). To further confirm this hypothesis, the local environment of the encapsulated Ru in the faujasite was studied by extended X-ray absorption fine structure (EXAFS) (Figure 2d), which revealed that the Ru center is surrounded by six nitrogen atoms. Ru−Cl interactions were not observed, indicating that either the deprotonated zeolite framework or outer sphere Cl atoms provide electroneutrality of the complex. The signals at higher radial distances (2−3 Å) originate from the well-ordered carbon atoms of the bipy ligands. The intensity of these signals is similar as for the molecular complex (Ru(bipy)$_3$Cl$_2$), which is another indication that the Ru-atom is attached to three bipy ligands. Furthermore, the formation of Ru(bipy)$_3^{2+}$ was also confirmed in very good yields by XAS calculations (Figure S7 and Table S2), and a good fit was obtained between the measured spectrum of the EMC-1-Ru and the simulated spectrum of the encapsulated Ru(bipy)$_3^{2+}$ with interatomic Ru−N and Ru−C distances of 2.09 and 2.9 Å, respectively (Figure S8).

Optimizing the Reaction Conditions. The performance of the single-site heterogeneous catalyst, EMC-1-Ru, for the trifluoromethylation of arenes was tested by employing 1,2-dimethoxybenzene (veratrole) as model substrate, trifluoro-

methanesulfonyl chloride (CF$_3$SO$_2$Cl) as trifluoromethylation agent, Mg acetate (Mg(OAc)$_2$) as base, and water to increase the base's solubility under the optimized reaction conditions (Table 1, entry 1).

Table 1. Performance of the Catalyst for the Trifluoromethylation of the Model Substrate Veratrole (3c) under Different Conditions
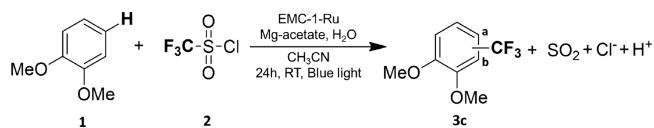
entry	conditions	yield 3c (Y_1^b/Y_2^c) (%)
1	optimized conditions^a	85/9
2	0 eq Mg(OAc)$_2$^{d}	78/6
3	1 eq Mg(OAc)$_2$	82/10
4	5 eq Mg(OAc)$_2$	82/8
5	0 μL H$_2$O	47/4
6	30 μL H$_2$O	70/6
7	120 μL H$_2$O^d	78/10
8	2 eq CF$_3$SO$_2$Cl	57/2
9	10 eq CF$_3$SO$_2$Cl^d	74/20
10	15 h reaction^a	78/4
11	48 h reaction^a	76/17
12	no catalyst	<1
13	no light	<1

^{a}**1** (0.1 mmol), **2** (5 eq), Mg(OAc)$_2$ (2 eq), H$_2$O (60 μL), EMC-1-Ru (1 mol % Ru), and 1 mL MeCN, blue light (455−470 nm, 40 W), 24 h at room temperature. $^b Y_1$ is the yield of the product with one CF$_3$-group at position a or b. $^c Y_2$ is the yield of the products with 2x CF$_3$-groups. ^{d}Catalyst is not crystalline anymore.

To verify the role of the catalyst, control experiments in the absence of catalyst or light were executed, and the lack of product under these conditions proves the photocatalytic role of EMC-1-Ru (Table 1, entries 12 and 13). Organic nitrogen bases, such as pyridine and trimethylamine, are not preferred to trap the HCl formed in the trifluoromethylation reaction since undesired reactions were detected (Table S3).[6] Inorganic bases, on the other hand, were more promising, and in particular, the acetate bases were good candidates with regard to their pK_b and high water solubility (Tables S4 and S5). The highest yield (94%) was obtained when using Mg(OAc)$_2$. Although a good product yield was also observed in the absence of base, the zeolite catalyst was unstable and could not be recycled (Figure S9).[32] Consequently, next to proton abstraction from the product intermediate,[6] the base is also required to control the reaction environment. Nevertheless, an excessively large amount of Mg(OAc)$_2$ has a negative impact on the atom economy since more waste is generated while the product yield (90%) remains unchanged (Table 1, entries 2−4). Generally, an increase of product yield was noticed upon the addition of water due to a higher base solubility (Table 1, entries 5−7). However, an elevated H$_2$O content decreases the catalyst's stability (HCl and CF$_3$SO$_3$H formation; Figures S10 and S12). By increasing the amount of trifluoromethylating agent (Table 1, entries 8 and 9), the yield increased to 94%, but at 10 eq of CF$_3$-source, catalyst decomposition and excessive amounts of undesired double-trifluoromethylated products were observed (Figure S11). Furthermore, the optimal reaction time was estimated at 24 h by a kinetic study since at shorter times, the reaction had not yet reached

its maximal conversion. However, prolongation beyond 24 h did not increase the product yield, and more difunctionalized products were observed (Table 1, entries 10 and 11, and Figure S13).

The faujasite-type material EMC-1 is used as the support material for the synthesis of the solid single-site catalyst. This zeolite (SAR = 3.6)[27] not only has suitable cage dimensions to host the molecular trifluoromethylation catalyst; it also withstands the acidified environment as confirmed by the PXRD data (Figure S14). The conventional NaY zeolite (CBV-100, SAR = 2.5) has a significantly lower SAR; it is not an appropriate support for the reaction since pore collapse due to excessive dealumination (Figure 3) and concomitant
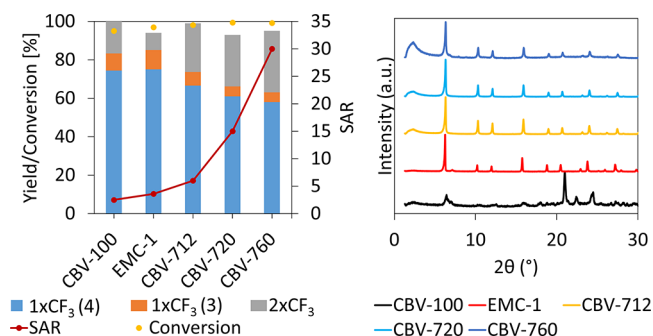

Figure 3. The reaction yield/conversion of zeolite supports with different SAR ratios (red line) (CBV-100 (SAR = 2.5), EMC-1 (SAR = 3.6), CBV-712 (SAR = 6), CBV-720 (SAR = 15), and CBV-760 (SAR = 30)). 1,2-Dimethoxy-4-trifluoromethylbenzene ($1xCF_3$ (**4**)) is displayed in blue, 1,2-dimethoxy-3-trifluoromethylbenzene ($1xCF_3$ (**3**)) is displayed in orange, and double-trifluoromethylated ($2xCF_3$) products are displayed in gray (left). PXRD diffractogram of the different support materials after the reaction to check the crystallinity of the material (right).

leaching are observed (Table S6). On the other hand, commercial zeolites with a higher SAR ratio (e.g., CBV-712 with a Si/Al ratio of 6 as well as CBV-720 and CBV-760 with even higher Si/Al ratios) were more stable, and the crystallinity of the zeolites was preserved (Figure 3). However, in this latter scenario, leaching of the Ru complex was also noted (Table S6). Typically, these high SAR zeolites are produced from NaY during a steaming process, during which water is responsible for gradually etching away the aluminum from the framework, resulting in defects and mesopores.[33,34] Consequently, part of the photocatalyst is trapped in these mesopores with less pore size restriction (Figure S15 and Table S7), and this ultimately caused Ru leaching. Note also that the EMC-1-Ru material produced the highest selectivity for mono-trifluoromethylated products.

Catalyst Heterogeneity/Stability. A recyclability test demonstrates that 95% of the catalyst's activity is retained toward mono-trifluoromethylated product after three recycling runs, while a small decrease in initial reaction rate is observed (Figure 4 and Figure S15). Moreover, the total amount of Ru leaching in the reaction mixture after three runs is estimated at 3.5% (Table S8), and the PXRD patterns at the end of the recyclability test did not show a significant decrease in crystallinity for the EMC-1 support (Figure 4). Additionally, a filtration test was executed (Figure S17) where the filtrate was collected after 4 h; it showed no additional yield after 24 h, while ICP analysis of the reaction mixture showed only 1.4% leaching, which is likely attributed to the fine fraction of the
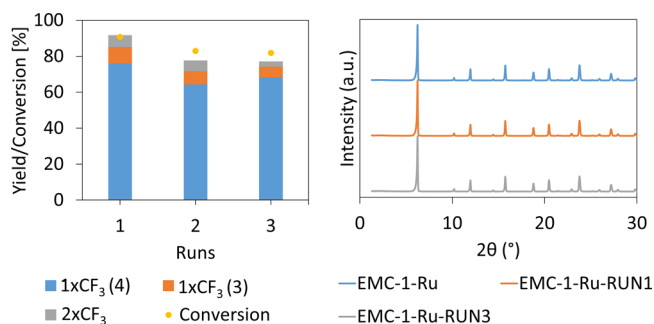

Figure 4. Recyclability test for three consecutive runs. A small reduction in yield was observed after three experiments (left). XRD diffractogram of the loaded EMC-1-Ru, the supporting material, after one run and after three runs (right). After the reaction, the mixture was centrifuged, the reaction solution was removed, and the zeolite was washed several times by Milli-Q water and dried under vacuum overnight. Subsequently, fresh reaction mixture was added to the zeolite, and a second/third reaction run was performed. The reaction was performed as follows: veratrole (0.1 mmol), CF_3SO_2Cl (5 eq), $Mg(OAc)_2$ (2 eq), H_2O (60 μL), EMC-1-Ru (1 mol % Ru), and 1 mL MeCN, blue light (455–470 nm, 40 W), 24 h at room temperature.

zeolite powder (Table S9). Furthermore, EXAFS data of the single-site catalyst after reaction illustrate a slight decrease in the Ru–N signal (Figure S18 and Table S10). Consequently, less than 5% of the active Ru(II) is deactivated.

Substrate Scope. This mild, visible light-induced trifluoromethylation procedure was then applied to different (hetero)-arenes to investigate the scope of this single-site heterogeneous catalyst (Figure 5). Low yields are observed for arenes bearing electron-withdrawing groups (**3a**, 4%), since the aromatic ring is poorly activated for the electrophilic CF_3 radical. On the contrary, electron-donating substituents have a remarkable positive effect on the product yield. Therefore, we turned our attention to more electron-rich arenes, resulting in trifluoromethylated products with good to excellent yields. However, phenol (**3h**) as substrate has a moderate yield of 36% of the ortho-trifluoromethylated product due to problems with limited selectivity, radical polymerization, and subsequent pore blockage in the zeolite. A set of different heterocycles (**3d**–**3g**) was tested with the knowledge that there is an unmet need for CF_3 functionalization procedures for these useful pharmacophores. As shown in Figure 5, these heteroarenes are also suitable reactants in this trifluoromethylation protocol (**3d**–**3g**, 22–89%). As a rule, the most electron-rich position of the arene is preferentially trifluoromethylated (**3c**, **3d**, **3g**, **3i**–**k**, **3n**, and **3o**).[2,6,35] The amount of double-trifluoromethylated product was extremely high for 1,3,5-trimethoxybenzene (**3m**) due to the strongly electron-donating character of the three methoxy groups. Finally, the trifluoromethylation of relevant compounds such as 3,4-dimethoxybenzoic acid (**3o**) revealed the practicality of this approach.[6]

Finally, pharmaceutically relevant substrates were selected to demonstrate the significance of the single-site heterogeneous catalyst for the pharmaceutical and fine chemical industry (Figure 6). Product **3p** has a similar molecular structure as its RNA base analog, uracil, and is obtained with excellent yield and selectivity. Furthermore, **3q** and **3r** with methoxymethyl (MOM)-protecting groups are attractive as precursor materials for the synthesis of uridine derivatives, which have excellent antiviral and cancer-treating properties (e.g., trifluridine is a drug used against the herpes virus). Therefore, large uridine-
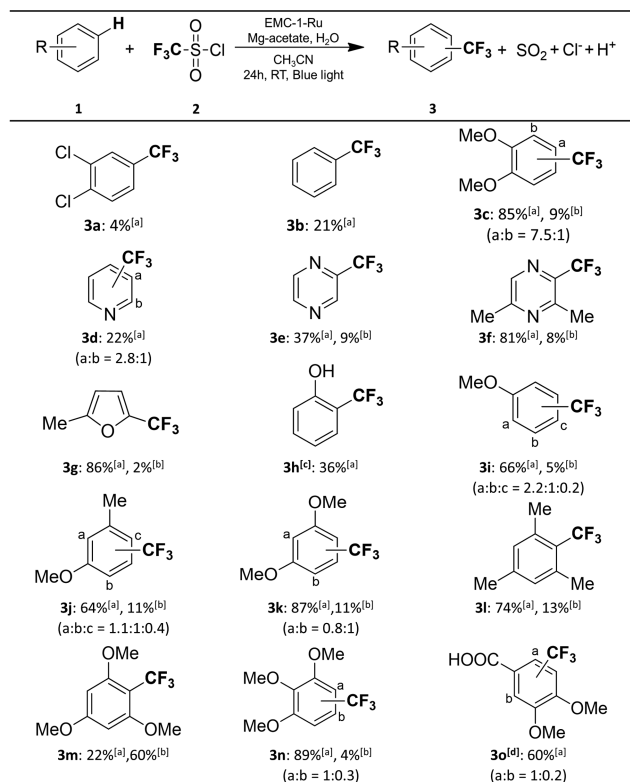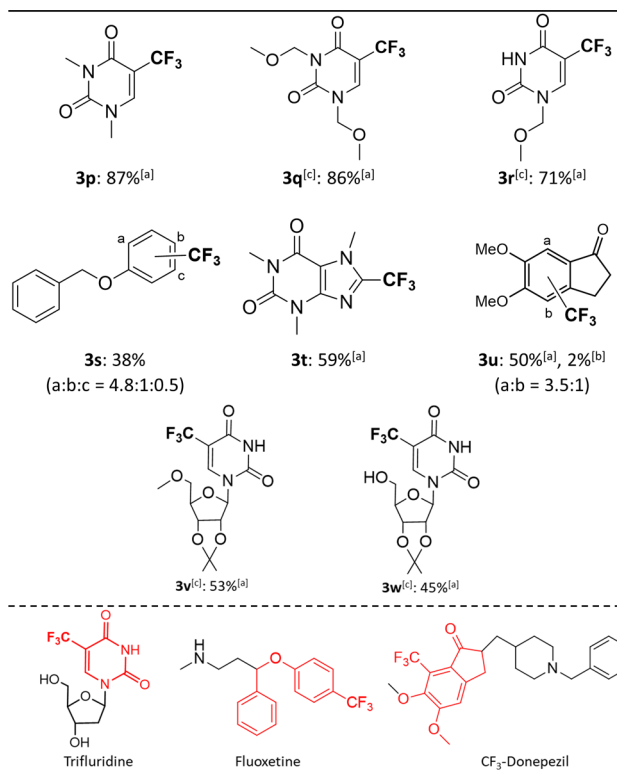
[a]The yield of the products with one CF₃-group, the ratio of the products of trifluoromethylation at the respective positions is given between brackets. [b]The yield of the products with two CF₃-groups. [c]Poor mass balance due to polymerization reactions. [d]The yield is determined by ¹⁹F-NMR.

Figure 5. Substrate scope. Reaction conditions: **1** (0.1 mmol), **2** (5 eq), Mg(OAc)$_2$ (2 eq), H$_2$O (60 μL), EMC-1-Ru (1 mol % Ru), and 1 mL MeCN, blue light (455−470 nm, 40 W), 24 h at room temperature.

[a]The yield of the products with one CF₃-group, the selectivity for these products are showed between the brackets. [b]The yield of the products with two CF₃-groups. [c]The yield is determined by ¹⁹F-NMR.

Figure 6. Substrate scope of synthetically interesting substrates. Reaction conditions: substrate (0.1 mmol), CF$_3$SO$_2$Cl (5 eq), Mg(OAc)$_2$ (2 eq), H$_2$O (60 μL), EMC-1-Ru (1 mol % Ru), and 1 mL MeCN, blue light (455−470 nm, 40 W), 24 h at room temperature.

like substrates (**3v** and **3w**) were tested, and good yields/selectivities were obtained. The bulkiness of these molecules indicate that interactions between the substrate and the CF$_3$ radicals can be established at the surface of the zeolite support. Consequently, this trifluoromethylation protocol is also amenable toward larger substrates. Furthermore, the precursor for the antidepressant drug fluoxetine (**3s**, 38%), the biologically active heteroarene caffeine (**3t**, 59%), and the anti-Alzheimer precursor (**3u**, 50%) were trifluoromethylated with good yields.

CONCLUSIONS

In this work, we have developed a convenient photoredox-based method for the heterogeneous trifluoromethylation of arenes. The photoactive complex Ru(bipy)$_3^{2+}$ is entrapped in the supercages of the highly stable zeolite EMC-1, and the complex formation was successfully confirmed by FTIR, UV−Vis, and XAS. Various zeolite supports with different SAR ratios were screened, and an optimal SAR ratio and zeolite architecture were identified for which a good catalyst stability is combined with a high activity. Moreover, the reaction can be performed efficiently under mild reaction conditions and under visible-light irradiation with CF$_3$SO$_2$Cl as economically interesting trifluoromethylating agent. Additionally, the heterogeneity of the single-site catalyst was confirmed via recycling tests, and metal analysis of the reaction mixture indicated that leaching of the Ru complex was very limited. Finally, the substrate scope revealed that this heterogeneous catalyst is

suitable for late-stage trifluoromethylation of industrially relevant arenes.

ASSOCIATED CONTENT

ⓈI Supporting Information

The Supporting Information is available free of charge at https://pubs.acs.org/doi/10.1021/acsami.1c19655.

> Detailed experimental procedures, optimization of the reaction conditions, kinetic experiments, additional characterization data (PDF)

AUTHOR INFORMATION

Corresponding Author

Dirk E. De Vos − *Centre For Membrane Separations, Adsorption, Catalysis, and Spectroscopy for Sustainable Solutions (cMACS), KU Leuven, Leuven 3001, Belgium;* ⓞ orcid.org/0000-0003-0490-9652; Email: dirk.devos@ kuleuven.be

Authors

Vincent Lemmens − *Centre For Membrane Separations, Adsorption, Catalysis, and Spectroscopy for Sustainable Solutions (cMACS), KU Leuven, Leuven 3001, Belgium*

Christophe Vos − *Centre For Membrane Separations, Adsorption, Catalysis, and Spectroscopy for Sustainable Solutions (cMACS), KU Leuven, Leuven 3001, Belgium*

Aram L. Bugaev − *The Smart Materials Research Institute, Southern Federal University, Rostov-on-Don 344090, Russia;* ⊚ orcid.org/0000-0001-8273-2560

Jannick Vercammen − *Centre For Membrane Separations, Adsorption, Catalysis, and Spectroscopy for Sustainable Solutions (cMACs), KU Leuven, Leuven 3001, Belgium*

Niels Van Velthoven − *Centre For Membrane Separations, Adsorption, Catalysis, and Spectroscopy for Sustainable Solutions (cMACs), KU Leuven, Leuven 3001, Belgium;* ⊚ orcid.org/0000-0003-3224-0239

Jorge Gascon − *King Abdullah University of Science and Technology (KAUST), Thuwal 23955, Saudi Arabia;* ⊚ orcid.org/0000-0001-7558-7123

Author Contributions

The manuscript was written through contributions of all authors. All authors have given approval to the final version of the manuscript.

Notes

The authors declare no competing financial interest.

ABBREVIATIONS

ET, electron transfer
SSA, specific surface area
bipy, 2,2′-bipyridine
SAR, silica-to-alumina ratio
TM, transition metal
SMR, substrate-to-metal ratio
MOM, methoxymethyl

REFERENCES

(1) Purser, S.; Moore, P. R.; Swallow, S.; Gouverneur, V. Fluorine in Medicinal Chemistry. *Chem. Soc. Rev.* **2008**, *37*, 320−330.

(2) Lin, J.; Li, Z.; Kan, J.; Huang, S.; Su, W.; Li, Y. Photo-driven Redox-neutral Decarboxylative Carbon-hydrogen Trifluoromethylation of (Hetero)arenes with Trifluoroacetic Acid. *Nat. Commun.* **2017**, *8*, 1−7.

(3) Furuya, T.; Kamlet, A. S.; Ritter, T. Catalysis for Fluorination and Trifluoromethylation. *Nature* **2011**, *473*, 470−477.

(4) Barata-Vallejo, S.; Postigo, A. New Visible-Light-Triggered Photocatalytic Trifluoromethylation Reactions of Carbon−Carbon Multiple Bonds and (Hetero) Aromatic Compounds. *Chem. - A Eur. J.* **2020**, *26*, 11065−11084.

(5) Beatty, J. W.; Douglas, J. J.; Cole, K. P.; Stephenson, C. R. J. A Scalable and Operationally Simple Radical Trifluoromethylation. *Nat. Commun.* **2015**, *6*, 1−6.

(6) Nagib, D. A.; Macmillan, D. W. C. Trifluoromethylation of Arenes and Heteroarenes by Means of Photoredox Catalysis. *Nature* **2011**, *480*, 224−228.

(7) Bottecchia, C.; Martín, R.; Abdiaj, I.; Crovini, E.; Alcazar, J.; Orduna, J.; Blesa, M. J.; Carillo, J. R.; Prieto, P.; Noël, T. De novo Design of Organic Photocatalysts: Bithiophene Derivatives for the Visible-light Induced C−H Functionalization of Heteroarenes. *Adv. Synth. Catal.* **2019**, *361*, 945−950.

(8) Kino, T.; Nagase, Y.; Ohtsuka, Y.; Yamamoto, K.; Uraguchi, D.; Tokuhisa, K.; Yamakawa, T. Trifluoromethylation of Various Aromatic Compounds by CF_3I in the Presence of Fe(II) Compound, H_2O_2 and Dimethylsulfoxide. *J. Fluorine Chem.* **2010**, *131*, 98−105.

(9) Charpentier, J.; Früh, N.; Togni, A. Electrophilic Trifluoromethylation by Use of Hypervalent Iodine Reagents. *Chem. Rev.* **2015**, *115*, 650−682.

(10) Barata-Vallejo, S.; Lantaño, B.; Postigo, A. Recent Advances in Trifluoromethylation Reactions with Electrophilic Trifluoromethylating Reagents. *Chem. - A Eur. J.* **2014**, *20*, 16806−16829.

(11) Liu, X.; Xu, C.; Wang, M.; Liu, Q. Trifluoromethyltrimethylsilane: Nucleophilic Trifluoromethylation and Beyond. *Chem. Rev.* **2015**, *115*, 683−730.

(12) Koike, T.; Akita, M. Fine Design of Photoredox Systems for Catalytic Fluoromethylation of Carbon-Carbon Multiple Bonds. *Acc. Chem. Res.* **2016**, *49*, 1937−1945.

(13) Chachignon, H.; Guyon, H.; Cahard, D. CF_3SO_2X (X = Na, Cl) as Reagents for Trifluoromethylation, Trifluoromethylsulfenyl-, −sulfinyl- and -sulfonylation and Chlorination. Part 2: Use of CF3SO2Cl. *Beilstein J. Org. Chem.* **2017**, *13*, 2800−2818.

(14) Guyon, H.; Chachignon, H.; Cahard, D. CF_3SO_2X (X = Na, Cl) as Reagents for Trifluoromethylation, Trifluoromethylsulfenyl-, −sulfinyl- and -sulfonylation. Part 1: Use of CF_3SO_2Na. *Beilstein J. Org. Chem.* **2017**, *13*, 2764−2799.

(15) Yin, D.; Su, D.; Jin, J. Photoredox Catalytic Trifluoromethylation and Perfluoroalkylation of (Hetero)Arenes Using Trifluoroacetic and Related Carboxylic Acids. *SSRN Electron J.* **2020**, DOI: 10.2139/ssrn.3606764.

(16) Bazyar, Z.; Hosseini-Sarvari, M. Au@ZnO Core-Shell: Scalable Photocatalytic Trifluoromethylation Using CF_3CO_2Na as an Inexpensive Reagent under Visible Light Irradiation. *Org. Process Res. Dev.* **2019**, *23*, 2345−2353.

(17) Baar, M.; Blechert, S. Graphitic Carbon Nitride Polymer as a Recyclable Photoredox Catalyst for Fluoroalkylation of Arenes. *Chem - A Eur. J.* **2015**, *21*, 526−530.

(18) Verified Market Research. *Global synthetic zeolite market - market size, status and forecast to 2027*; 2019.

(19) Corma, A.; Garcia, H. Zeolite-based Photocatalysts. *Chem. Comm.* **2004**, 1443−1459.

(20) Taira, N.; Saitoh, M.; Hashimoto, S.; Moon, H. R.; Yoon, K. B. Effect of Electron-acceptor Strength of Zeolite on the Luminescence Decay Rate of $Ru(bpy)_3^{2+}$ Incorporated within Zeolites. *Photochem. Photobiol. Sci.* **2006**, *5*, 822−827.

(21) Park, Y. S.; Lee, E. J.; Chun, Y. S.; Yoon, Y. D.; Yoon, K. B. Long-lived Charge-separation by Retarding Reverse Flow of Charge-balancing Cation and Zeolite-encapsulated $Ru(bpy)_3^{2+}$ as Photosensitized Electron Pump from Zeolite Framework to Externally Placed Viologen. *J. Am. Chem. Soc.* **2002**, *124*, 7123−7135.

(22) Binder, F.; Calzaferri, G.; Gfeller, N. Dye Molecules in Zeolites as Artificial Antenna. *Sol. Energy Mater. Sol. Cells* **1995**, *38*, 175−186.

(23) Sykora, M.; Maruszewski, K.; Treffert-Ziemelis, S. M.; Kincaid, J. R. A Synthetic Strategy for the Construction of Zeolite-entrapped Organized Molecular Assemblies. Preparation and Photophysical Characterization of Interacting Adjacent Cage Dyads Comprised of Two Polypyridine Complexes of Ru(II). *J. Am. Chem. Soc.* **1998**, *120*, 3490−3498.

(24) Moissette, A.; Hureau, M.; Col, P.; Vezin, H. Photoinduced Electron Transfers after t-stilbene Incorporation in Zeolite. Effect of the Presence of an Electron Acceptor on the Reactivity. *Microporous Mesoporous Mater.* **2017**, *254*, 128−135.

(25) García, H.; Roth, H. D. Generation and Reactions of Organic Radical Cations in Zeolites. *Chem. Rev.* **2002**, *102*, 3947−4008.

(26) DeWilde, W.; Peeters, G.; Lunsford, J. H. Synthesis and Spectoscopic Properties of Tris(2,2′-bipyridine)ruthenium(II) in Zeolite Y. *J. Phys. Chem.* **1980**, *84*, 2306−2310.

(27) Daou, T. J.; Dhainaut, J.; Chappaz, A.; Bats, N.; Harbuzaru, B.; Chaumeil, H.; Defoin, A.; Rouleau, L.; Patarin, J. The Use of Original Structure-Directing Agents for the Synthesis of EMC-1 Zeolite. *Oil Gas Sci. Technol.* **2015**, *70*, 447−454.

(28) Lainé, P.; Lanz, M.; Calzaferri, G. Limits of the in Situ Synthesis of Tris(2,2′-bipyridine)ruthenium(II) in the Supercages of Zeolite Y. *Inorg. Chem.* **1996**, *35*, 3514−3518.

(29) Munshi, M. U.; Martens, J.; Berden, G.; Oomens, J. Vibrational Spectra of the Ruthenium-Tris-Bipyridine Dication and Its Reduced Form in Vacuo. *J. Phys. Chem. A.* **2020**, *124*, 2449−2459.

(30) Komaty, S.; Özçelik, H.; Zaarour, M.; Ferre, A.; Valable, S.; Mintova, S. Ruthenium Tris(2,2′-bipyridyl) Complex Encapsulated in Nanosized Faujasite Zeolite as Intracellular Localization Tracer. *J. Colloid Interface Sci.* **2021**, *581*, 919−927.

(31) Prier, C. K.; Rankic, D. A.; MacMillan, D. W. C. Visible Light Photoredox Catalysis with Transition Metal Complexes: Applications in Organic Synthesis. *Chem. Rev.* **2013**, *113*, 5322−5363.

(32) Chandu, P.; Ghosh, K. G.; Das, D.; Sureshkumar, D. Photoredox Catalysed Allylic Trifluoromethylation via Ring Opening of Vinyl Cyclopropanes Using Langlois Reagent. *Tetrahedron* **2019**, *75*, 130641.

(33) Lutz, W.; Rüscher, C. H.; Gesing, T. M.; Stöcker, M.; Vasenkov, S.; Freude, D.; Gläser, R.; Berger, C. Investigations of the Mechanism of Dealumination of Zeolite Y by Steam: Tuned Mesopore Formation versus the Si/Al Ratio. *Stud. Surf. Sci. Catal.* **2004**, *154*, 1411−1417.

(34) Beyerlein, R. A.; Choi-feng, c.; Hall, J. B.; Huggins, B. J.; Ray, G. J. Effect of Steaming on the Defect Structure and Acid Catalysis of Protonated Zeolites. *Top. Catal.* **1997**, *4*, 27−42.

(35) Cui, L.; Matusaki, Y.; Tada, N.; Miura, T.; Uno, B.; Itoh, A. Metal-Free Direct C-H Perfluoroalkylation of Arenes and Hetero-arenes Using a Photoredox Organocatalyst. *Adv. Synth. Catal.* **2013**, *355*, 2203−2207.